Astronomy & Astrophysics manuscript no. output
July 6, 2026

N-body modelling of the ED-2 stream progenitor shows *Gaia* BH3's formation involved dynamical interactions

Daniel Marín Pina[1,2,3], Mark Gieles[2,4,5], Sara Rastello[2,3], Clàudia Garcia-Diago[2,3], Giuliano Iorio[2,3], and Marc Ardèvol[2,3]

1 Zentrum für Astronomie der Universität Heidelberg, Institut für Theoretische Astrophysik, Albert-Ueberle-Str. 2, 69120 Heidelberg
e-mail: daniel.marin@uni-heidelberg.de
2 Institut de Ciències del Cosmos (ICCUB), Universitat de Barcelona (UB), c. Martí i Franqués, 1, 08028 Barcelona, Spain
3 Departament de Física Quàntica i Astrofísica (FQA), Universitat de Barcelona (UB), Martí i Franquès 1, 08028 Barcelona, Spain
4 ICREA, Pg. Lluís Companys 23, 08010 Barcelona, Spain
5 Institut d'Estudis Espacials de Catalunya (IEEC), Edifici RDIT, Campus UPC, 08860 Castelldefels (Barcelona), Spain

Received XX; accepted XX

ABSTRACT

Context. The *Gaia* collaboration announced the discovery of a binary of a massive black hole ($33\,M_{\odot}$) with a low-mass giant star (*Gaia* BH3) in the ED-2 stellar stream. The properties of this binary, as well as its position in the stream, challenge a formation scenario invoking only isolated binary evolution.

Aims. We aim to quantify the importance of cluster dynamics in the formation of *Gaia* BH3 in the progenitor cluster of the ED-2 stream.

Methods. We performed detailed *N*-body simulations of the progenitor cluster of the ED-2 stream, including the effects of single and binary stellar evolution. We compared these simulations to observations of the ED-2 stream and the properties of *Gaia* BH3.

Results. We determine that *Gaia* BH3 most likely formed as an exchange binary that underwent multiple strong dynamical interactions. We highlight the importance of cluster dynamics in assembling *Gaia* BH3 and disfavour a formation scenario where it evolved unperturbed by dynamical interactions.

Conclusions. The role of dynamics should be considered when interpreting the properties of the population of star–black hole binaries found in the next *Gaia* data release.

Key words. Stars: black holes – binaries: general – globular clusters: individual: ED-2 progenitor – Methods: numerical

1. Introduction

Traditionally, observational evidence of (stellar-origin) black holes (BHs) came from X-ray binaries (Corral-Santana et al. 2016). This method is biased towards detecting binaries that are sufficiently tight to allow mass transfer from the star to the BH. In the last decade, most of the known BHs have been detected through gravitational wave (GW) emission (The LIGO Scientific Collaboration et al. 2025). These are produced in the last fractions of a second before a binary BH (BBH) merges, so the observational bias towards close binaries is even more dramatic.

Recently, we have begun to uncover a population of BHs that do not merge or accrete; they are 'dormant' BHs. One of the methods for detecting dormant BHs is in star–BH (S-BH) binaries via astrometry, measuring the perturbation of the parallax and proper motion of the companion star. In this regard, the *Gaia* mission has been key to uncovering these systems, with confirmed detections of three dormant BHs, named *Gaia* BH1 (El-Badry et al. 2023b; Chakrabarti et al. 2023), *Gaia* BH2 (El-Badry et al. 2023a), and *Gaia* BH3 (Gaia Collaboration et al. 2024). Many more such systems are expected to be discovered in the upcoming fourth *Gaia* Data Release (DR4). On top of these, other dormant S-BH binaries have been discovered with other methods, such as spectroscopy (VFTS 243 by Shenar et al. 2022; NGC 3201_12560 by Giesers et al. 2018, 2019; HD 130298 by Mahy et al. 2022; NGC 1850 BH1 by Saracino et al. 2022, 2023 — but see El-Badry & Burdge 2022 — and *Gaia* DR3 3425577610762832384, not yet confirmed, by Wang et al. 2024), lensing (OGLE-2011-BLG-0462; Lam et al. 2022), and most recently, *Hubble* and JWST astrometry (Whitaker et al. 2026)[1].

The properties and orbits in the Galactic plane of *Gaia* BH1 and *Gaia* BH2 are consistent with formation in star clusters (Rastello et al. 2023; Di Carlo et al. 2024; Tanikawa et al. 2024; Arca Sedda et al. 2024), isolated stellar binaries (Kotko et al. 2024; Mapelli et al. 2026), or stellar triples (Li et al. 2026). Both *Gaia* BH1 and *Gaia* BH2 have relatively light BHs ($\lesssim 10\,M_{\odot}$), mildly metal-poor companions ($[Fe/H] \sim -0.2$), and orbit in the Galactic plane. Compared to these, the properties and Galactic orbit of *Gaia* BH3 stand out. This binary consists of a massive BH ($m_{BH} = 33\,M_{\odot}$) and an extremely metal-poor ($[Fe/H] = -2.56$), low-mass ($m_{\star} = 0.76\,M_{\odot}$) giant star. The binary has a long period ($P = 4 \times 10^3$ d) and has an eccentricity of $e = 0.7$. *Gaia* BH3 is remarkably close to the Sun (590 pc), in an orbit in the Milky Way (MW) halo associated with the ED-2 stellar stream, which probably formed from a now-dissolved star cluster (Balbinot et al. 2023). The association with the stream is both kinematical and chemical (Balbinot et al. 2024; Hackshaw et al. 2025; Vanden Broeck et al. 2026). The mass of the BH is much higher than any other (stellar-origin) BH detected in the

[1] See mkenne15.github.io/BHCAT for an updated list of dormant BHs.

Article published by EDP Sciences, to be cited as https://doi.org/10.1051/0004-6361/202660620

MW, and is close to the median BH mass detected via GWs (see Fig. 3 in Marín Pina et al. 2024). This binary bridges the populations of BHs detected via electromagnetic measurements and GWs; hence, understanding its formation pathway can provide constraints on the populations of binaries with BHs and on the formation of GW sources.

There are two proposed explanations for the origin of *Gaia* BH3: either it formed from the isolated evolution of a binary of stars (see e.g. Iorio et al. 2024; El-Badry 2024) or it formed via dynamical interactions in the progenitor cluster of the ED-2 stream (Marín Pina et al. 2024). Both of these channels would likely result in no chemical peculiarities of the *Gaia* BH3 star with respect to other stars in ED-2, in line with recent chemical analyses (e.g. Hackshaw et al. 2025; Vanden Broeck et al. 2026). The fact that *Gaia* BH3 is associated with the ED-2 stream provides circumstantial evidence that dynamics played a role in shaping its present-day properties but does not rule out a binary origin unperturbed by dynamics. We modelled the collisional dynamics of the progenitor cluster of the ED-2 stream to quantify the effect of dynamics in the formation of *Gaia* BH3. A preliminary analysis of the results presented hereafter was presented in Marín Pina et al. (2025).

In Sect. 2 we describe the *N*-body models used to simulate the ED-2 stream progenitor. In Sect. 3 we study the stream formation in our simulations and constrain the cluster's initial parameters with the observed *Gaia* data. In Sect. 4 we explore the most likely origin of *Gaia* BH3, including the hypothesis that it is a triple system with an inner BBH. In Sect. 5 we characterise the formation environment of S-BH binaries in our simulations. In Sects. 6 and 7 we discuss and summarise our findings.

2. Methods

We performed a set of simulations of the ED-2 progenitor cluster using the high-performance *N*-body code PETAR (Wang et al. 2020a). PETAR uses a hybrid method to integrate the evolution of dense collisional systems, which separates the long- and short-range interactions. The former are evolved using a Barnes-Hut particle-tree method (Barnes & Hut 1986) with a second-order leapfrog integrator; the latter are integrated using a fourth-order Hermite method with slowdown-algorithmic regularisation (SDAR; Wang et al. 2020b). The SDAR method uses a change of coordinates to avoid singularities in Newtonian gravity (algorithmic regularisation; Kustaanheimo & Stiefel 1965) together with a time scaling ('slowdown'; Mikkola & Aarseth 1996), which is used to efficiently compute the perturbation of a binary over several orbits. This method allows us to avoid the computational cost and numerical instability caused by having very small timesteps. With this hybrid formalism (particle-tree and SDAR), we can efficiently simulate star clusters with a significant binary population.

The initial conditions for the cluster simulations were set up using the MCLUSTER code (Küpper et al. 2011). We initialised all models using a Plummer (1911) density profile with a Kroupa (2001) initial mass function between $0.08\,M_\odot$ and $150\,M_\odot$. The initial mass and half-mass density of the ED-2 progenitor, M_0 and $\rho_{h,0}$, are not known. Our approach is to fix the (approximate) dissolution time of the cluster to $t_{dis} \in [0.5, 4, 8]$ Gyr, for different combinations of M_0 and $\rho_{h,0}$. The method used to compute them is explained in Appendix A. The range in masses of all models is within the constraints imposed by Balbinot et al. (2024), namely $M_0 \gtrsim 2\times10^3\,M_\odot$ (such that at least one massive star that can create a BH is sampled from the initial mass function) and $M_0 \lesssim 5.2\times10^4\,M_\odot$ (because of the negligible scatter in light element abundances).

These models were run both with and without a primordial binary population. Hereafter, we use the term 'primordial' to refer to binaries that originated as part of the cluster formation process. For the models with primordial binaries, we used 100% binary fraction among stars above $5\,M_\odot$, using the Sana et al. (2012) period and eccentricity distributions. We acknowledge that this is a mild extrapolation of primary masses with respect to their sample and is on the higher end of initial binary fraction. For lower-mass stars, we used the Duquennoy & Mayor (1991) period distribution and a thermal eccentricity distribution, with a total binary fraction of $f_b = 0.4$. The low- and high-mass stars are paired in binaries separately, and thus we did not allow extreme-mass-ratio binaries at the beginning of the simulation (the minimum mass ratio at zero-age main sequence is 1/30, larger than that required to form *Gaia* BH3). This choice, motivated by the data showing that O and B stars are more likely to be found in equal-mass binaries (Sana & Evans 2011), is discussed in Sect. 6.1. We assumed that the clusters have a single population of stars, with metallicity equal to that of the *Gaia* BH3 star, [Fe/H] = −2.56 ($Z \simeq 6\times10^{-5}$). The initial parameters of the cluster models are summarised in Table 1.

Once the models were set up, we evolved them using PETAR until 13 Gyr. Due to the low metallicity, we performed the single and binary stellar evolution with the BSEEMP code (Tanikawa et al. 2020, 2022). We assumed that compact object formation follows the rapid supernova mechanism of Fryer et al. (2012), with a strong pulsational pair instability cutoff (Belczynski et al. 2016). Overall, our models have a range from a few to a hundred BHs.

In order to include the effect of the MW tidal field on the clusters, PETAR can interface with GALPY (Bovy 2015), a code library used to model Galactic dynamics. In our simulations, the clusters were evolved in a MW-like potential using the MWPOTENTIAL2014 routine. The initial conditions are such that, after 13 Gyr, the centre of density of the cluster (modelling it as a test particle) matches the current position of *Gaia* BH3 in the sky. In the following section, we relax this assumption and consider shifts of an extra $\Delta t \leq 100$ Myr in the orbital evolution. The Galactic orbital elements were computed using GALPY and the PETAR prescriptions for the Sun's position and velocity, and shown in Table 2.

3. Formation of the ED-2 stream

To verify that our simulations are representative of the progenitor cluster of the ED-2 stream, we compared the streams formed in our simulations to the ED-2 *Gaia* data reported in Balbinot et al. (2023). Since the cluster is old ($t \gtrsim 13$ Gyr; Balbinot et al. 2024), it must have undergone several orbits around the MW. There are many uncertainties associated with the evolution of the Galactic potential, so our goal is not to match the shape of the observed stream exactly, but rather to show that our models dissolve and form a structure similar to ED-2.

Since the cluster is completely dissolved, we expect that most of the stars will have dispersed through the Galaxy and have very faint magnitudes. To account for detectability, we converted the output of our simulations (based on the radii and luminosities of the stars from BSEEMP) to the *Gaia* *G* magnitudes. We first computed the bolometric magnitude and then used the $B-V$ colour correction from Flower (1996) and Torres (2010) and the $G-V$ corrections from Jordi et al. (2010). We then limited our sample to stars within the *G* magnitude limits in the ED-2 sample

Table 1: Initial parameters of the cluster simulations: model name, (approximate) dissolution time t_{dis} (computed according to Appendix A), half-mass density $\rho_{h,0}$, mass M_0, binary fraction f_b, and number of runs with different random seeds N_{runs}.

Model name	t_{dis} [Gyr]	$\rho_{h,0}$ [$M_\odot$ pc^{-3}]	M_0 [$M_\odot$]	f_b	N_{runs}
TD8_HiRHO_WBIN	8	760	7.7×10^3	0.4	10
TD8_HiRHO_NOBIN				0.0	10
TD8_LoRHO_WBIN	8	240	3.9×10^4	0.4	10
TD8_LoRHO_NOBIN				0.0	10
TD4_HiRHO_WBIN	4	760	2.7×10^3	0.4	10
TD4_HiRHO_NOBIN				0.0	10
TD4_LoRHO_WBIN	4	240	1.4×10^4	0.4	10
TD4_LoRHO_NOBIN				0.0	10
TD0.5_VLoRHO_WBIN	0.5	25	3.5×10^3	0.4	10

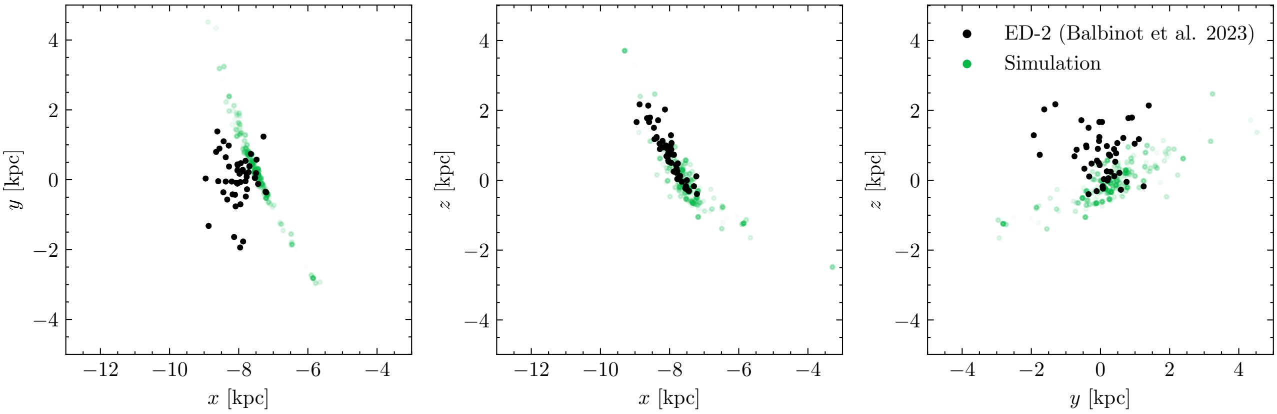

Fig. 1: Positions of the stars of the ED-2 stream in Galactocentric Cartesian coordinates. The *Gaia* data from Balbinot et al. (2023) are shown in black. A run of the TD8_LoRHO_NOBIN model is shown in green, with each star coloured according to its magnitude. The cluster is shown at the end of the simulation (13 Gyr), which was set up such that the centre of mass of the cluster matches the observed current position of *Gaia* BH3.

Table 2: Initial Galactic orbit of the cluster at the start of the simulation, derived from backtracking the estimated Galactic orbit of *Gaia* BH3 in the MWPOTENTIAL2014 potential, assuming it matches the position of the centre of mass of the cluster at $t = 13$ Gyr.

	$t = 13$ Gyr	$t = 0$
Galactocentric x [kpc]	-7.63	-0.222
Galactocentric y [kpc]	0.466	-8.23
Galactocentric z [kpc]	-0.022	-2.98
Galactocentric v_x [km/s]	121	266
Galactocentric v_y [km/s]	-280	164
Galactocentric v_z [km/s]	-134	19.3
Orbital SMA a [kpc]	17.1	
Orbital eccentricity e	0.616	
Radial period T_p [Myr]	406	

from Balbinot et al. (2023). For illustrative purposes, in Fig. 1 we show the Galactocentric positions of the members of ED-2 (Balbinot et al. 2023) superimposed on the final snapshot of one of our simulations (TD8_LoRHO_NOBIN).

Per Mikkola et al. (2023), the ED-2 stream is expected to contain roughly $N_{vis} = 180$ observable members within 3 kpc from the Sun (which are not found because of the lack of radial velocity measurements). This estimate is obtained with a data-driven maximum penalised-likelihood algorithm, allowing the authors to obtain the number of stars in the stream while lacking full radial velocity measurements. In Fig. 2a we compare their value for N_{vis} to what is found in the final snapshot of each of our simulations. We preface our analysis of this comparison by stating that the $N_{vis} = 180$ value is a rough estimate; as such, we used it as a 'sanity-check' verification. Furthermore, we note that the stream formation process is stochastic and, as such, we did not aim for an exact match, just qualitative agreement. From this comparison, we see that the most massive models are preferred by the data. The low-density, early dissolution model (TD0.5_VLoRHO_*) results in too low N_{vis}, and thus we excluded it from further analysis.

To construct Fig. 2a, we assumed that the observed Galactocentric position of *Gaia* BH3 corresponds to the centre of the stream. While this is approximately true for the observed stars, it might not be the case for the complete stream. To ensure that our conclusions are independent of this choice, we evolved the stream for an additional 100 Myr (about a quarter of the radial period), taking 10000 snapshots per model, equally spaced in time. For illustrative purposes, we show one such snapshot in Fig. 3 (from model TD8_HiRHO_NOBIN, after 37 Myr), chosen such that N_{vis} is equal to the value found in Mikkola et al. (2023). In Fig. 2b we show N_{vis} for these snapshots, separated by the initial parameters. A similar conclusion can be drawn as for

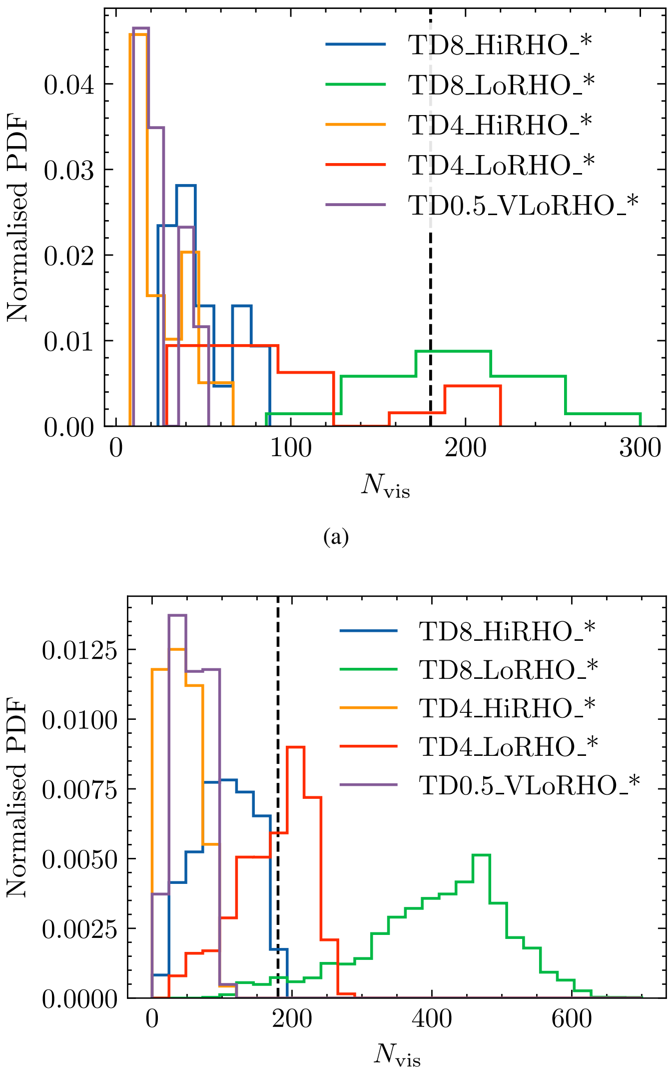

Fig. 2: Probability density function of the number of visible sources in the stream, separated by the initial conditions of the simulations. *Panel (a)*: Obtained at the end of the simulation (13 Gyr). *Panel (b)*: Obtained from snapshots uniformly spaced in the 100 Myr after the end of the simulation. The models with and without primordial binaries are binned. The dashed black line marks $N_{\rm vis}$ = 180 (Mikkola et al. 2023).

Fig. 2a: the more massive clusters are preferred over lower-mass clusters.

4. The origin of *Gaia* BH3

In the previous section, we show that our models of globular clusters dissolve in the *Gaia* BH3 orbit and form streams similar to ED-2, therefore lending support to the hypothesis that *Gaia* BH3 formed in the ED-2 progenitor cluster. In a cluster, we distinguish the following formation channels for *Gaia* BH3:

- Primordial: The binary originated as part of the cluster formation process, but interactions with other stars, BHs, and binaries altered its properties (period and eccentricity) significantly.
- Exchange: The star or BH formed in a primordial binary but exchanged its companion via dynamical interactions.
- Dynamical: The binary was assembled from a previously unbound star and a BH (or its progenitor star) via dynamical interactions.
- Isolated: The binary originated as part of the cluster formation process and evolved unperturbed by dynamical interactions.

In Sect. 4.1 we explore the S-BH systems formed in the first three scenarios, and obtain the most likely formation channel for *Gaia* BH3 in a dynamical environment. In Sect. 4.2 we explore the last scenario, quantifying whether dynamical interactions have a significant effect on the formation of S-BH systems in the ED-2 stream progenitor.

4.1. Formation of *Gaia* BH3 in the ED-2 progenitor

In this section we estimate the likelihood of the first three formation scenarios (primordial, exchange and dynamical). We extracted the data for these scenarios from the S-BH formed in our cluster simulations, defined as bound S-BH pairs present at the final snapshot (after 13 Gyr of evolution), irrespective of their properties or location in the stream. For the primordial and exchange formation channels, we used the cluster models with primordial binaries (*_WBIN), separating the S-BH binaries depending on whether they were paired up at the beginning of the simulation. For the dynamical formation scenario, we used our models without primordial binaries (*_NOBIN). In Fig. 4 we show the distribution of properties of the S-BH binaries in our models, separated by formation channel. In Fig. 5 we show the same data but separated by M_0, $\rho_{\rm h,0}$, and $t_{\rm dis}$, using cumulative histograms due to low-number statistics. In both these figures, we exclude the low-density models (TD0.5_VLoRHO_WBIN) since they cannot reproduce the observed ED-2 stream data.

To discern the most likely formation scenario, we computed the posteriors $P({\rm prim}\,|\,{\rm G}_3)$, $P({\rm exc}\,|\,{\rm G}_3)$, and $P({\rm dyn}\,|\,{\rm G}_3)$, with ${\rm G}_3 = \{\log P, e, q\}$ the measured parameters of *Gaia* BH3. Each of these represents the probability that *Gaia* BH3 formed in its respective scenario. Using Bayesian statistics, we have

$$P({\rm dyn}\,|\,{\rm G}_3) = \frac{P({\rm G}_3\,|\,{\rm dyn})P({\rm dyn})}{P({\rm G}_3)} \quad (1)$$

with

$$P({\rm G}_3) = P({\rm G}_3\,|\,{\rm prim})P({\rm prim}) + P({\rm G}_3\,|\,{\rm exc})P({\rm exc}) + P({\rm G}_3\,|\,{\rm dyn})P({\rm dyn}). \quad (2)$$

Here, P(prim), P(exc), and P(dyn) are the fraction of S-BH binaries formed in our simulations for each of the three channels, and are taken as priors. The priors P(prim), P(exc) are computed by dividing the total number of S-BH systems formed in the primordial and exchange channels (respectively) by the number of *_WBIN clusters in our simulations. The prior P(dyn) is computed by dividing the total number of dynamical S-BH systems in the *_NOBIN simulations by the number of these simulations. $P({\rm G}_3\,|\,{\rm dyn})$ is the probability density function (PDF) of the parameters found in the dynamical channel, evaluated at ${\rm G}_3$. The PDF is computed via a kernel density estimation using Gaussian kernels with a bandwidth estimated with Silverman's criterion. The posteriors for the other channels, $P({\rm prim}\,|\,{\rm G}_3)$ and $P({\rm exc}\,|\,{\rm G}_3)$, are computed using the same approach.

On average, there are significantly more S-BH systems in clusters with primordial binaries (see Table 3). While we expected this to depend on the initial binary fraction, we find

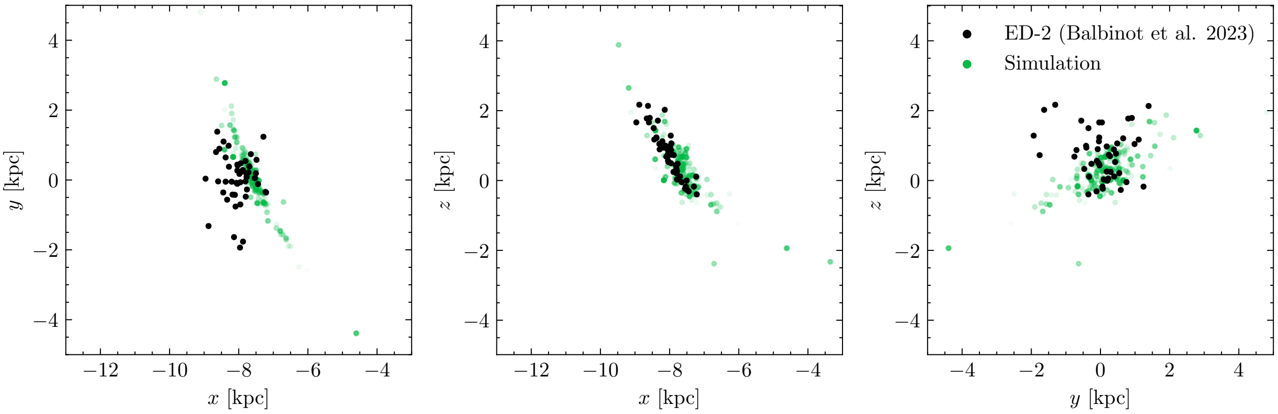

Fig. 3: Positions of the stars of the ED-2 stream in Galactocentric Cartesian coordinates. *Gaia* data from Balbinot et al. (2023) are in black. A run of the TD8_HiRHO_NOBIN model is shown in green, with each star coloured according to its magnitude. The cluster is shown 37 Myr after the end of the simulation to maximise visual similarity to the ED-2 stream.

P(prim) ≫ P(dyn) and P(exc) ≫ P(dyn) (i.e. the rate of formation of dynamical binaries is very low). We show this in Fig. 6 and discuss it below. In our Bayesian analysis, the posteriors are $P(\mathrm{exc}\,|\,\mathrm{G}_3) = 0.79$, $P(\mathrm{prim}\,|\,\mathrm{G}_3) = 0.18$ and $P(\mathrm{dyn}\,|\,\mathrm{G}_3) = 0.03$. These are the probabilities that *Gaia* BH3 formed in each of the three channels, accounting for both the formation rates and the measured parameters (period, eccentricity, and mass ratio). Although the parameters of *Gaia* BH3 are slightly better reproduced in a dynamical formation scenario (as was found in Marín Pina et al. 2024), the low efficiency of models without primordial binaries at producing S-BH binaries means that the dynamical formation scenario is disfavoured. Overall, our models show a preference for *Gaia* BH3 being formed as an exchange binary.

In our simulation with binaries, all the BH progenitor stars are originally paired in primordial binaries. This is due to our choice of initial conditions that forces a 100% binary fraction for stars above 5 $\mathrm{M}_\odot$. Within the exchange channel, we find that most of our S-BH binaries (∼ 95%) form from a BH (or a binary containing a BH) that interacts with a low-mass stellar binary, exchanging the companion star and forming a dormant S-BH.

Table 3: Average number of S-BH binaries per cluster at the end of the simulation $\langle N_{\mathrm{S-BH}}\rangle$, separated by cluster model.

Model name	$\langle N_{\mathrm{S-BH}}\rangle$
TD8_HiRHO_WBIN	1.5
TD8_HiRHO_NOBIN	0.2
TD8_LoRHO_WBIN	7.4
TD8_LoRHO_NOBIN	0.2
TD4_HiRHO_WBIN	0.9
TD4_HiRHO_NOBIN	0.1
TD4_LoRHO_WBIN	2.0
TD4_LoRHO_NOBIN	0.3
TD0.5_VLoRHO_WBIN	1.2

Furthermore, we can use the observed properties of *Gaia* BH3 to constrain the initial properties of the ED-2 stream progenitor. Qualitatively, the data shown in Fig. 5 hint at a preference towards the massive ($M_0 \geq 1.4 \times 10^4\,\mathrm{M}_\odot$) models with intermediate values of the initial density ($\rho_{\mathrm{h},0} = 240\,\mathrm{M}_\odot\,\mathrm{pc}^{-3}$); mostly due to the positive scaling of $\langle N_{\mathrm{S-BH}}\rangle$ with initial cluster mass (Table 1 and 3). This preference agrees with the results of the comparison with the ED-2 stream in Sect. 3. While the most massive cluster models (TD8_LoRHO_WBIN) produce a handful of S-BH binaries ($\langle N_{\mathrm{S-BH}}\rangle \simeq 7.4$; see Fig. 3), most of these will not be detectable due to their distance to the Sun (because of the fanning of the stream) and *Gaia* observational cuts.

In general, S-BH binaries are rare sources in clusters. In Fig. 6 we show the efficiency, η, defined as the average number of S-BH per cluster (at 13 Gyr) per unit of initial cluster mass. Our simulations with primordial binaries have a few (∼ 1 − 4) of these binaries per cluster (see Fig. 3), whereas models without primordial binaries typically produce one or none. We conclude that we do not expect to detect other S-BH binaries in the ED-2 stream. Including primordial binaries increases efficiency by an order of magnitude; as mentioned above, we expect the formation rates to depend on the initial binary fraction. While our models predict that the efficiency is a slowly decreasing function of mass, we do not recover the scaling in Marín Pina et al. (2024), i.e. $\eta \propto M^{-1.2} r_{\mathrm{v}}^{-0.42}$ with r_{v} the initial virial radius. Instead, we find $\eta \propto M^{-0.5} r_{\mathrm{v}}^{-0.1}$. This can be attributed to different choices of the initial conditions. For example, their models start with $\rho_{\mathrm{h},0} \sim 10^{3-6}\,\mathrm{M}_\odot\,\mathrm{pc}^{-3}$ and much higher masses ($M_0 \sim 10^{5-6}\,\mathrm{M}_\odot$). Compared to our models ($\rho_{\mathrm{h},0} < 10^3\,\mathrm{M}_\odot\,\mathrm{pc}^{-3}$), they explore a different regime for the early dynamics of the cluster.

4.2. Could *Gaia* BH3 have formed in isolation?

In the previous section we show that *Gaia* BH3 likely formed as an exchange binary in the ED-2 progenitor cluster. We next test the effect that dynamical interactions in the cluster had on shaping the properties of primordial binaries. This is akin to asking how the properties of *Gaia* BH3 are affected by dynamical interaction after it formed from binary evolution (as proposed in e.g. Iorio et al. 2024; El-Badry 2024; Mapelli et al. 2026).

To quantify the effect of dynamical interactions on S-BH properties, we extracted all binaries at the beginning of our cluster simulations and evolved them in isolation (i.e. unperturbed by cluster dynamics). We used the same binary stellar evolution code and prescriptions as in the cluster simulations so that all differences are strictly due to dynamical interactions. In Fig. 4 we show the distributions of the properties of the S-BH systems formed in our simulations, separated by formation channels and including those binaries evolved without the effects of cluster dynamics (i.e. in isolation). We have also included the systems evolved in isolation in Fig. 5.

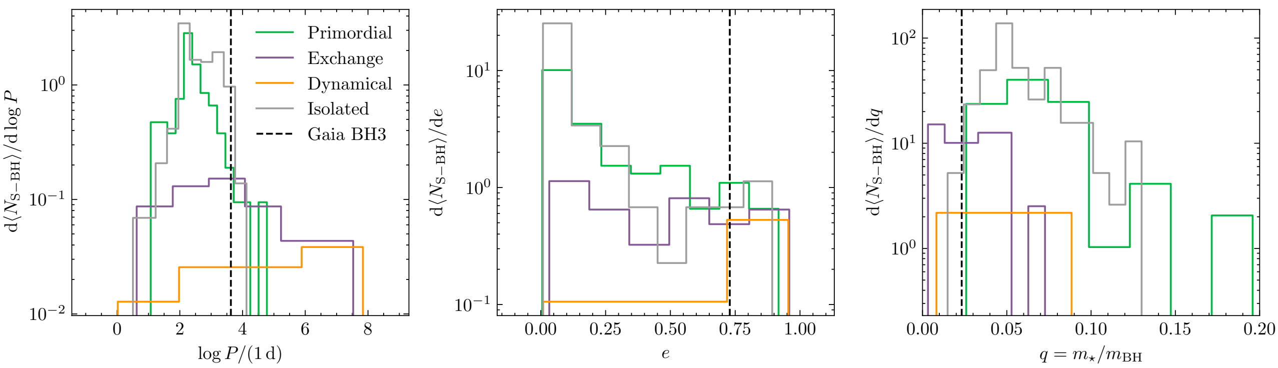

Fig. 4: Probability density function of the number of S-BH binaries in our simulations as a function of the logarithm of the period (*left*), the eccentricity (*middle*), and the mass ratio (*right*). The vertical scale is normalised such that the area under the histogram equals the average number of S-BH binaries per cluster. In green, purple, and orange we show a S-BH formed in the primordial, exchange, and dynamical channel, respectively. The primordial binaries that evolved in isolation are shown in grey (isolated channel), and the parameters of *Gaia* BH3 as the dashed black line.

We find that dynamics significantly modifies the S-BH binaries formed in the cluster models. In those with primordial binaries, at the end of the simulation, there are $\sim$ 22% fewer S-BH binaries than would be present if the binaries evolved in isolation. From Fig. 4, disruptions affect long-period binaries the most. Dynamics leads to a marginal reduction of the number of S-BH binaries, but a significant change in their properties.

Furthermore, in Fig. 7, we show the number of strong interactions, N_{int}, that each S-BH has undergone by the end of the simulations. We define strong interactions as those that undergo SDAR (see Wang et al. 2020b and Sect. 2). For a binary of mass m_{b} with a perturber of mass m_{p}, this is implemented when the distance from the perturber to the closest member of the binary, r_{p}, satisfies the following condition:

$$r_{\mathrm{p}} < \left(\frac{2m_{\mathrm{p}}}{m_{\mathrm{b}}\gamma_{\mathrm{min}}}\right)^{1/3} R, \tag{3}$$

where R is the closest distance along the perturber's trajectory and $\gamma_{\mathrm{min}} = 1.5$ a free coefficient. For binary-single interactions, the median value is $N_{\mathrm{int}} = 19$, while for more chaotic binary-binary interactions, $N_{\mathrm{int}} = 3$. We can further this analysis by limiting our sample to S-BH binaries with a period similar to *Gaia* BH3. If we apply a conservative cut of $10^3 < P/(1\,\mathrm{d}) < 10^5$, we find a median of $N_{\mathrm{int}} = 28$ for three-body interactions and $N_{\mathrm{int}} = 1$ for four-body interactions. The difference is not significant, which can be interpreted as the maximum and minimum periods for S-BH binaries being the tails of the N_{int} distribution. The number of strong interactions highlight the importance of dynamics and disfavour an isolated approach to studying the formation of *Gaia* BH3.

We next analysed the effect of the initial conditions of the cluster models on N_{int} (Fig. 8). If we focus on three-body interactions, we can see a larger N_{int} in the models with a larger dissolution time, and only a small correlation with density. Indeed, by instead analysing $N_{\mathrm{int}}/t_{\mathrm{dis}}$, we drove the models together, with the main difference between them being the initial density. Furthermore, the gap in the N_{int} cumulative distribution caused by the difference in initial density is higher in models with a larger dissolution time. We note that this applies only to S-BH binaries that survive until the end of the simulations and that the cluster may have had S-BH binaries that underwent more interactions, but those binaries were disrupted or merged and thus are not present in our sample.

As an interesting addendum, we note that strong interactions involving S-BH binaries may lead to observable transients such as micro-tidal disruption events (Perets et al. 2016; Rastello et al. 2026).

4.3. *Gaia* BH3 as a triple system

An alternative explanation for the nature of *Gaia* BH3 is that its 33 $\mathrm{M}_{\odot}$ BH is actually a BBH with a small semimajor axis (SMA). In this section, we study the formation of star–BBH (S-BBH) systems in our ED-2 progenitor models.

If we assume that *Gaia* BH3 is a S-BBH, there are some constraints on the possible ranges of SMA of the BBH orbit. First, if it is too small, the BBH will inspiral and merge due to GW emission. Our cluster simulations take this into account by implementing the orbit-averaged 2.5 post-Newtonian orbital shrinking (Peters equation; Peters 1964). Thus, if we find a S-BBH at the present time in our simulations, it has survived for long enough without merging. On the other side, the SMA of the BBH cannot be too large, as that would induce dynamical effects in the star that would have been detected by *Gaia* astrometry. Future observations can provide a stronger upper bound on the SMA of a possible inner binary.

In our simulations, we find a very small amount of S-BBH systems, with S-BH binaries being 40 times as common. Furthermore, none of the S-BBH systems has an outer orbit compatible with the observed properties of *Gaia* BH3, mostly because they have much longer periods. Therefore, our models disfavour the hypothesis that the unseen companion in *Gaia* BH3 is a BBH, in agreement with previous results (Tanikawa et al. 2025).

5. S-BH formation environment

In this section, we characterise the formation environment of the S-BH binaries in our simulations, i.e. their position, time, and dynamical hardness at the moment of formation. As before, we considered only the S-BH present at the end of our simulations (i.e. after 13 Gyr of evolution). First, we characterised the distribution of the radial position of S-BHs at formation, r_{form}. For each S-BH binary, we obtained the first snapshot they appear in and computed r_{form} from their distance to the density centre of the cluster, defined as in Casertano & Hut (1985). Results are shown in Fig. 9.

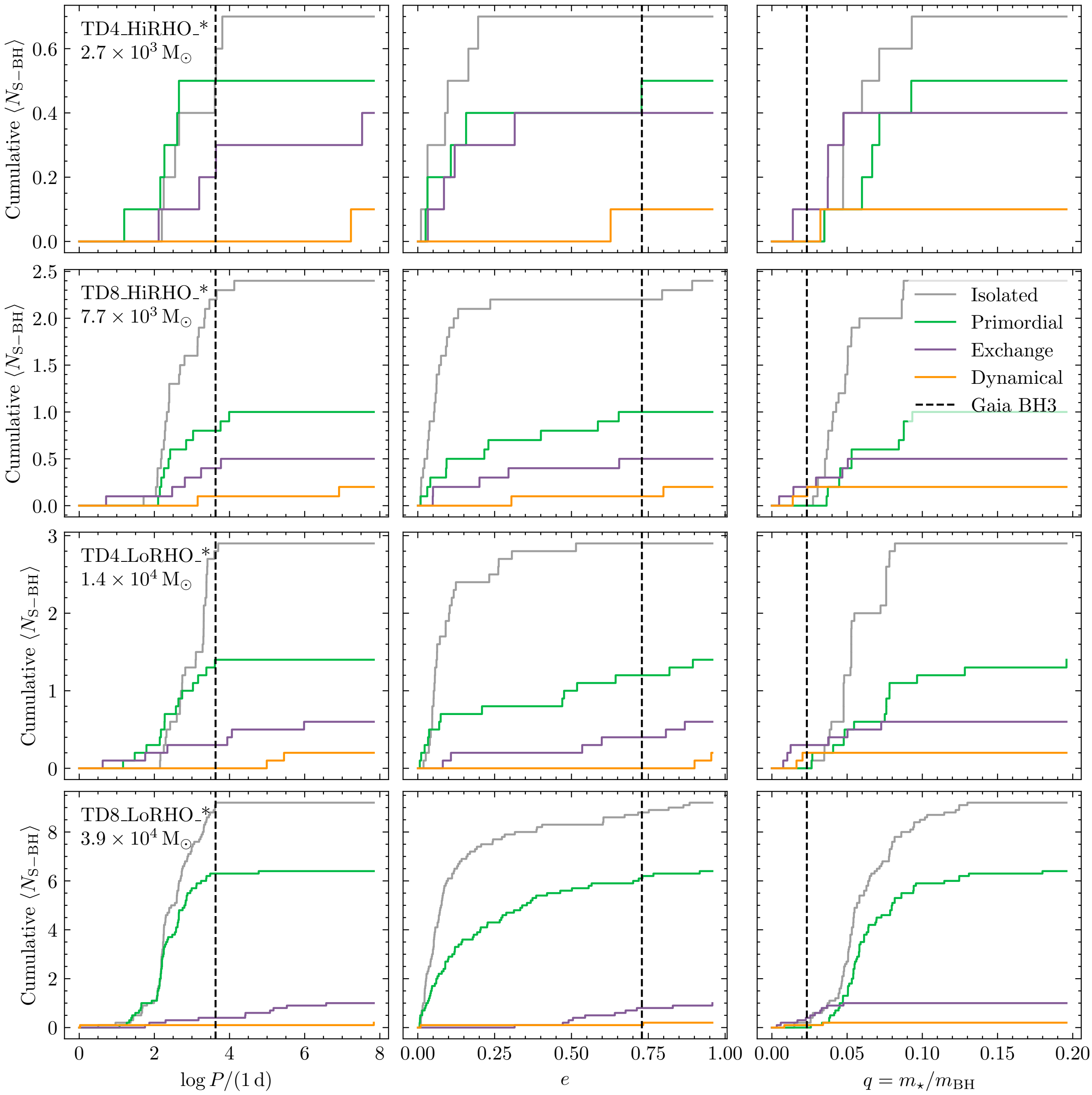

Fig. 5: Cumulative distribution of the properties of S-BH binaries in our simulations as a function of the logarithm of the period (*left*), the eccentricity (*middle*), and the mass ratio (*right*), separated by the initial conditions of the model. The vertical scale is normalised such that the rightmost value is the mean number of S-BH binaries in each cluster simulation for each channel, obtained by averaging over $N_{\rm runs}$. In green, purple, and orange we show a S-BH formed in the primordial, exchange, and dynamical channel, respectively. The primordial binaries that evolved in isolation are shown in grey (isolated channel), and the parameters of *Gaia* BH3 as the dashed black line.

For primordial binaries, the $r_{\rm form}$ distribution is simply the initial density profile of the cluster, with a median $r_{\rm form} \sim r_{\rm h}$, where $r_{\rm h}$ is the half-mass radius of the cluster. For the exchange binaries, their formation happens at a rate (per unit volume) of $\Gamma \sim n_{\rm BH} n_{\rm b} \Sigma v_{\rm rel}$, with $n_{\rm BH}$, $n_{\rm b}$ the local number density of stellar binaries and BHs, respectively; Σ their relative cross-section (usually estimated from Heggie et al. 1996), and $v_{\rm rel}$ their relative velocity. Around the central regions of the cluster, the density profile can be taken as roughly constant, so that Γ is roughly independent of the radial position. Then, the number of formed exchange S-BH binaries is $N_{\rm S-BH} \sim \Gamma r^3 \Delta t$, and thus the distribution of $r_{\rm form}$ is ${\rm d}N_{\rm S-BH}/{\rm d}r_{\rm form} \propto r^2$. However, at a certain radius, the density and interaction rates drop, thus producing the peak seen in Fig. 9. A similar argument can be made for dynamical binaries.

Next, we considered the formation time of S-BH binaries, $t_{\rm form}$. We defined it as the first snapshot in the simulations at which the star is paired in a binary with the BH (or its progenitor). For storage efficiency, we only saved snapshots every 100 Myr; however, the error introduced in this approach is $\lesssim 1\%$ of our simulation time. The distribution of $t_{\rm form}$ is shown in Fig. 10. Dynamical binaries have a roughly constant, low forma-

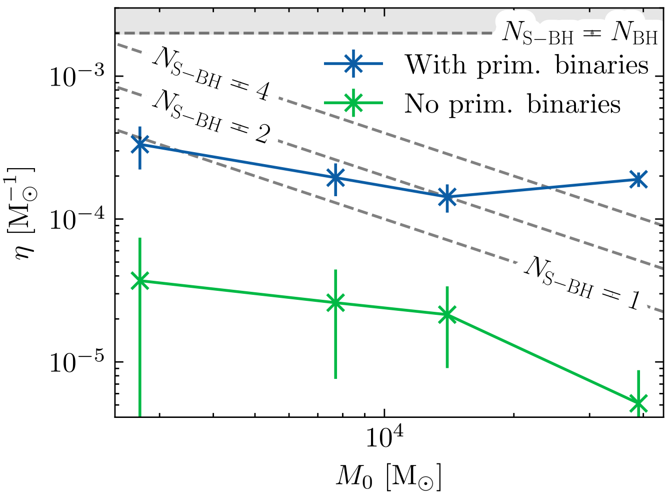

Fig. 6: Efficiency (η), defined as the number of S-BH binaries ($N_{\rm S-BH}$) per unit of initial cluster mass, as a function of the initial cluster mass. We show models with a primordial binary population in blue and models without primordial binaries in green. The error bars represent the standard error of the mean (of multiple N-body models), assuming $N_{\rm S-BH}$ behaves like a Poissonian variable.

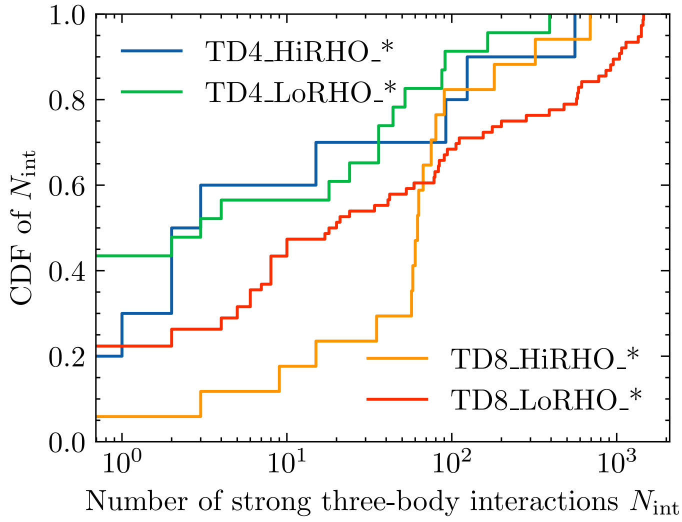

Fig. 8: Cumulative distribution function of the number of three-body interactions undergone by the S-BH binaries present at the end of our simulations, separated by the initial conditions of the cluster.

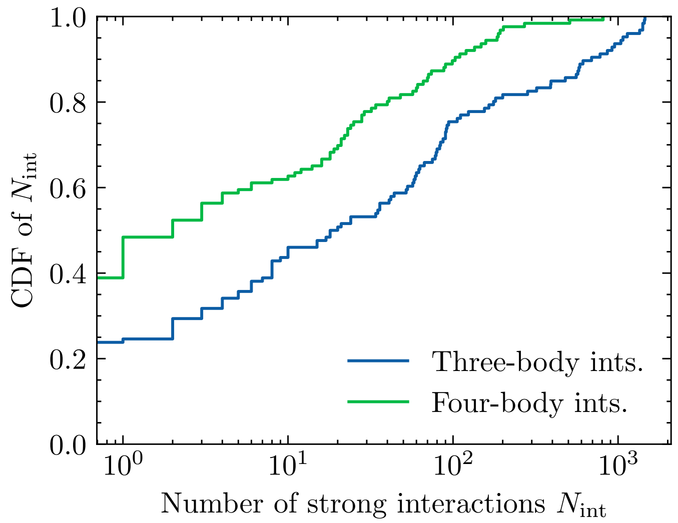

Fig. 7: Cumulative distribution function of the number of interactions undergone by the S-BH binaries present at the end of our simulations. Binary-single (three-body) interactions are shown in blue and binary-binary (four-body) interactions in green. The median value for three-body interactions is $N_{\rm int} = 18$, and for four-body interactions it is $N_{\rm int} = 3$

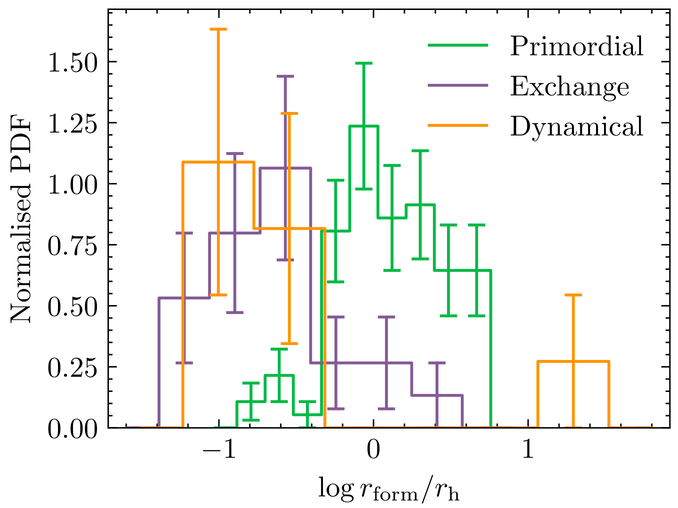

Fig. 9: Probability density function of the number of S-BH binaries in our simulations as a function of the logarithm of their formation radius (in units of the half-mass radius, $r_{\rm h}$), separated by formation channels. The vertical scale is normalised such that the area under the histogram is one. The uncertainties of each bin are computed as $\sqrt{N_{\rm S-BH}}$ within the bin.

tion rate; meanwhile, the formation of exchange binaries shows hints of peaking at earlier times.

An alternative formation channel suggests the possibility of assembling S-BH binaries in tidal tails (Peñarrubia 2021). In our set of simulations, we only find three S-BH binaries that become formally bound after cluster dissolution, with a SMA about 10^{2-3} times larger than that of *Gaia* BH3. While this is a promising formation pathway for wider binaries, we disfavour it as a formation channel of *Gaia* BH3.

Finally, we considered the hardness ratio, ϵ, of S-BH binaries in our simulation, defined as the ratio of the (absolute) binary binding energy to the average kinetic energy of stars in the central region of the cluster, both evaluated at the moment of formation. We computed it as $\epsilon = |E_{\rm b}| / \langle m\sigma^2 \rangle$, with $|E_{\rm b}| = G m_\star m_{\rm BH}/(2a)$, and $\langle m\sigma^2 \rangle$ computed within $r_{\rm h}$. The value of ϵ defines a transition in the stability of binaries in clusters: those with $\epsilon \lesssim 1$ (soft binaries) tend to disrupt due to the interaction with other stars or BHs, while binaries with $\epsilon \gtrsim 1$ (hard binaries) tend to get more bound after an interaction.

In Fig. 11 we show ϵ for all S-BH binaries in our simulations. We find that $\sim 90\%$ of the exchange binaries and $\sim 60\%$ of the dynamical binaries in our simulation form above the hard-soft boundary ($\epsilon \geq 1$). While soft binaries are likely formed at a much higher rate, they are easily ionised and thus do not survive

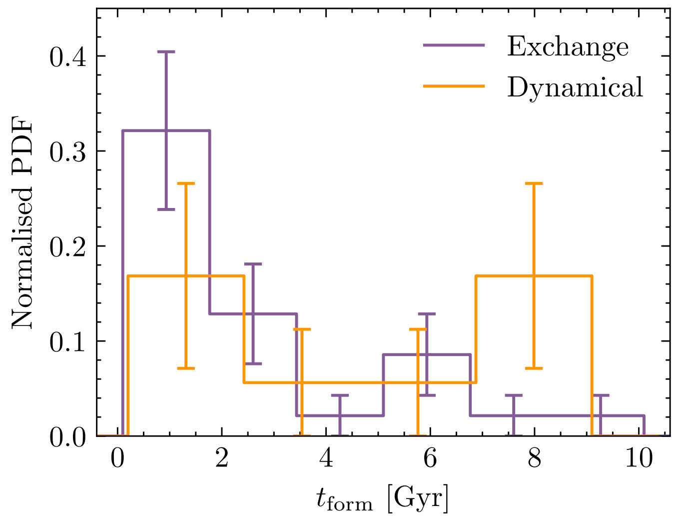

Fig. 10: Same as Fig. 9 but as a function of the S-BH binaries' formation time. Primordial S-BH binaries (not shown) form at $t = 0$.

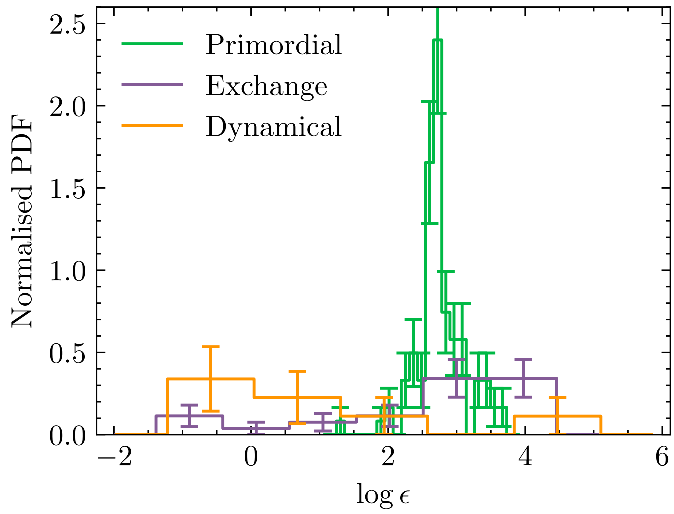

Fig. 11: Same as Fig. 9 but as a function of the logarithm of S-BH binaries' hardness ratio, ϵ.

to the end of the simulation. At the moment of cluster formation, the primordial binaries that will become primordial S-BHs are hard, with $\epsilon \sim 10^{2-3}$.

6. Discussion

6.1. Alternative binary evolution models

The use of different assumptions for stellar and binary evolution (including the properties of primordial binaries) in our cluster simulations would result in different values for the parameters of S-BH systems formed in our models. In this section we argue that the key points in this paper are independent of the assumed evolutionary models and initial conditions.

First, our models show that the most likely origin for *Gaia* BH3 is an exchange, which shows that the effect of dynamics is important for the formation of this binary. This discards the possibly unrealistic limit case with no primordial binaries. Furthermore, the comparison of the observable sources in our simulations (after detection cuts) to the stream data (Sect. 3) shows that the cluster had an initially high density, meaning that any S-BH binary still in the stream after multiple gigayears of evolution necessarily underwent multiple strong interactions (see Fig. 7). After these interactions, which include exchanges and resonances, the effect of the initial conditions for binaries is diluted.

Regarding the isolated scenario (where the binary evolved in the ED-2 progenitor unperturbed by dynamical interactions), we were not able to reproduce the mass ratio of *Gaia* BH3 due to our initial choice for the limits in the mass ratio distribution. Choosing different limits and other binary evolution models, it has been shown that it is possible to form *Gaia* BH3-like systems (El-Badry 2024; Iorio et al. 2024; Mapelli et al. 2026). However, our argument to disfavour an isolated origin of *Gaia* BH3 is based on the ionisation and overall difference of the S-BH systems with the input initial conditions due to cluster dynamics. Since *Gaia* BH3 formed in the ED-2 progenitor, it must have undergone multiple strong interactions whose effect cannot be neglected.

6.2. Uncertainties in the Galactic potential

In our simulations, we only considered a simplified model of the Galactic potential (MWPOTENTIAL2014; Bovy 2015). This potential is defined by a bulge with a power-law density profile with an exponential cut-off, a disk, and a dark-matter halo. However, it is axisymmetric and does not consider time evolution.

The use of that specific form of the potential is justified mainly by our ignorance about the time evolution of the true MW potential, together with computational constraints. Including irregularities in the potential would lead to a heating of the ED-2 stream in our simulations, which implies a greater fanning of the stars along the direction transverse to the principal axis of the stream. This would play a role in Fig. 1, which would bring the simulations closer to the observed data. Furthermore, this would lead to a shift of the distribution of $N_{\rm vis}$ in Fig. 2 to lower values, which only strengthens our conclusions that the ED-2 stream formed from a cluster with a high initial density.

7. Conclusions

We studied different formation mechanisms of *Gaia* BH3 in the progenitor cluster of the ED-2 stream. To do so, we used targeted N-body simulations of that cluster, including realistic single and binary stellar evolution models and the Galactic potential.

Regarding the stream formation, we show that the likely progenitor of the ED-2 stream is a now-dissolved star cluster, with an initial mass within the uncertainties presented in Balbinot et al. (2024), i.e. $2 \times 10^3 \lesssim M/{\rm M}_\odot \lesssim 5.2 \times 10^4$. The higher-mass limit is preferred, based on the number of visible sources in the stream. We show that this cluster dissolved after some gigayears of evolution, and a scenario where it had a very low initial density is disfavoured, as that would lead to a much sparser stream than what is found in the data.

Regarding the origin of *Gaia* BH3, we show that it likely formed from an exchange interaction between a BH and a primordial stellar binary of the ED-2 cluster, which had its properties significantly altered by subsequent interactions within the cluster environment. The probability that *Gaia* BH3 formed as a dynamical binary from a previously unbound BH and a single star is low. Furthermore, we show that the properties of primordial S-BH binaries in the ED-2 progenitor cluster are significantly modified by dynamical interactions, which challenges models that study the formation of *Gaia* BH3 in isolation. We also considered the possibility that *Gaia* BH3 is a triple system composed of an inner BBH with an outer star but find that this is an unlikely scenario, in line with previous studies.

Finally, we characterised the formation environment of S-BH binaries in our simulation, including their radial position, formation time, and binding energy. These results can be useful as hindsight for future studies targeting the formation of S-BH systems in clusters, including the potential for rapid population synthesis methods.

In summary, this paper shows that the most likely formation scenario for *Gaia* BH3 is a BH formed as part of a primordial binary that exchanged its companion star, then underwent multiple strong dynamical interactions. We highlight the importance of cluster dynamics in assembling *Gaia* BH3, and disfavour a formation scenario where it evolved unperturbed by strong dynamical interactions. Our work suggests that future studies interpreting the population of dormant S-BH binaries of the next *Gaia* data release cannot neglect the effects of cluster dynamics.

Acknowledgements. We thank Katie Breivik for insights regarding the isolated scenario. DMP thanks other participants in the KITP programme STELLARBH25 for useful discussions. DMP thanks Ugo di Carlo for his early involvement in the project. DMP thanks Ataru Tanikawa for insights regarding the S-BBH scenario. DMP acknowledges support from the Deutsche Forschungsgemeinschaft (DFG, German Research Foundation) through project number 546850815 (acronym: DoBlack) and under Germany's Excellence Strategy EXC 2181/1 - 390900948 (the Heidelberg STRUCTURES Excellence Cluster). This research was supported in part by grant no. NSF PHY-2309135 to the Kavli Institute for Theoretical Physics (KITP). DMP and MG acknowledge financial support from the grants PRE2020-091801, PID2024-155720NB-I00, CEX2024-001451-M, funded by MCIN/AEI/10.13039/501100011033 (State Agency for Research of the Spanish Ministry of Science and Innovation). SR acknowledges financial support from the Beatriu de Pinós postdoctoral fellowship program under the Ministry of Research and Universities of the Government of Catalonia (Grant Reference No. 2021 BP 00213). GI is supported by a fellowship grant from la Caixa Foundation (ID 100010434). The fellowship code is LCF/BQ/PI24/12040020.

References

Arca Sedda, M., Kamlah, A. W. H., Spurzem, R., et al. 2024, MNRAS, 528, 5119
Balbinot, E., Dodd, E., Matsuno, T., et al. 2024, A&A, 687, L3
Balbinot, E., Helmi, A., Callingham, T., et al. 2023, A&A, 678, A115
Barnes, J. & Hut, P. 1986, Nature, 324, 446
Belczynski, K., Holz, D. E., Bulik, T., & O'Shaughnessy, R. 2016, Nature, 534, 512
Bovy, J. 2015, ApJS, 216, 29
Casertano, S. & Hut, P. 1985, ApJ, 298, 80
Chakrabarti, S., Simon, J. D., Craig, P. A., et al. 2023, AJ, 166, 6
Corral-Santana, J. M., Casares, J., Muñoz-Darias, T., et al. 2016, A&A, 587, A61
Di Carlo, U. N., Agrawal, P., Rodriguez, C. L., & Breivik, K. 2024, ApJ, 965, 22
Duquennoy, A. & Mayor, M. 1991, A&A, 248, 485
El-Badry, K. 2024, The Open Journal of Astrophysics, 7, 38
El-Badry, K. & Burdge, K. B. 2022, MNRAS, 511, 24
El-Badry, K., Rix, H.-W., Cendes, Y., et al. 2023a, MNRAS, 521, 4323
El-Badry, K., Rix, H.-W., Quataert, E., et al. 2023b, MNRAS, 518, 1057
Flower, P. J. 1996, ApJ, 469, 355
Fryer, C. L., Belczynski, K., Wiktorowicz, G., et al. 2012, ApJ, 749, 91
Gaia Collaboration, Panuzzo, P., Mazeh, T., et al. 2024, A&A, 686, L2
Gieles, M. & Gnedin, O. Y. 2023, MNRAS, 522, 5340
Giesers, B., Dreizler, S., Husser, T.-O., et al. 2018, MNRAS, 475, L15
Giesers, B., Kamann, S., Dreizler, S., et al. 2019, A&A, 632, A3
Hackshaw, Z., Hawkins, K., & Manea, C. 2025, ApJ, 995, 140
Heggie, D. C., Hut, P., & McMillan, S. L. W. 1996, ApJ, 467, 359
Iorio, G., Torniamenti, S., Mapelli, M., et al. 2024, A&A, 690, A144
Jordi, C., Gebran, M., Carrasco, J. M., et al. 2010, A&A, 523, A48
Kotko, I., Banerjee, S., & Belczynski, K. 2024, MNRAS, 535, 3577
Kroupa, P. 2001, MNRAS, 322, 231
Küpper, A. H. W., Maschberger, T., Kroupa, P., & Baumgardt, H. 2011, MNRAS, 417, 2300
Kustaanheimo, P. E. & Stiefel, E. 1965, Journal für die reine und angewandte Mathematik (Crelles Journal), 1965, 204
Lam, C. Y., Lu, J. R., Udalski, A., et al. 2022, ApJ, 933, L23
Li, Z., Lu, X., Lü, G., et al. 2026, A&A, 706, A105
Mahy, L., Sana, H., Shenar, T., et al. 2022, A&A, 664, A159
Mapelli, M., Sgalletta, C., Müller-Horn, J., et al. 2026, arXiv e-prints, arXiv:2604.12839
Marín Pina, D., Gieles, M., Rastello, S., & Iorio, G. 2025, arXiv e-prints, arXiv:2510.07021
Marín Pina, D., Rastello, S., Gieles, M., et al. 2024, A&A, 688, L2
Mikkola, D., McMillan, P. J., & Hobbs, D. 2023, MNRAS, 519, 1989
Mikkola, S. & Aarseth, S. J. 1996, Celestial Mechanics and Dynamical Astronomy, 64, 197
Peñarrubia, J. 2021, MNRAS, 501, 3670
Perets, H. B., Li, Z., Lombardi, Jr., J. C., & Milcarek, Jr., S. R. 2016, ApJ, 823, 113
Peters, P. C. 1964, Physical Review, 136, 1224
Plummer, H. C. 1911, MNRAS, 71, 460
Rastello, S., Iorio, G., Gieles, M., & Wang, L. 2026, A&A, 707, A217
Rastello, S., Iorio, G., Mapelli, M., et al. 2023, MNRAS, 526, 740
Sana, H., de Mink, S. E., de Koter, A., et al. 2012, Science, 337, 444
Sana, H. & Evans, C. J. 2011, in IAU Symposium, Vol. 272, Active OB Stars: Structure, Evolution, Mass Loss, and Critical Limits, ed. C. Neiner, G. Wade, G. Meynet, & G. Peters, 474–485
Saracino, S., Kamann, S., Guarcello, M. G., et al. 2022, MNRAS, 511, 2914
Saracino, S., Shenar, T., Kamann, S., et al. 2023, MNRAS, 521, 3162
Shenar, T., Sana, H., Mahy, L., et al. 2022, Nature Astronomy, 6, 1085
Tanikawa, A., Cary, S., Shikauchi, M., Wang, L., & Fujii, M. S. 2024, MNRAS, 527, 4031
Tanikawa, A., Wang, L., Fujii, M. S., et al. 2025, The Open Journal of Astrophysics, 8, 79
Tanikawa, A., Yoshida, T., Kinugawa, T., Takahashi, K., & Umeda, H. 2020, MNRAS, 495, 4170
Tanikawa, A., Yoshida, T., Kinugawa, T., et al. 2022, ApJ, 926, 83
The LIGO Scientific Collaboration, the Virgo Collaboration, the KAGRA Collaboration, et al. 2025, arXiv e-prints, arXiv:2508.18082
Torres, G. 2010, AJ, 140, 1158
Vanden Broeck, G., Merle, T., Tan Mai, N., et al. 2026, arXiv e-prints, arXiv:2605.02353
Wang, L., Iwasawa, M., Nitadori, K., & Makino, J. 2020a, MNRAS, 497, 536
Wang, L., Nitadori, K., & Makino, J. 2020b, MNRAS, 493, 3398
Wang, S., Zhao, X., Feng, F., et al. 2024, Nature Astronomy, 8, 1583
Whitaker, M., Kerr, E., Seth, A., et al. 2026, arXiv e-prints, arXiv:2606.18350

Appendix A: Dissolution time

To find a combination of initial mass and half-mass density, $(M_0, \rho_{h,0})$, that results in a given dissolution time, t_{dis}, we used the expressions for t_{dis} of tidally limited clusters with BHs from Gieles & Gnedin (2023):

$$t_{dis} = 10\,\mathrm{Gyr}\frac{2/3}{y}\frac{30\,\mathrm{M}_\odot/\mathrm{Myr}}{\left|\dot{M}_{ref}\right|}\frac{0.32\,\mathrm{Myr}^{-1}}{\Omega_{tid}}\left(\frac{M_i}{2\times10^5\,\mathrm{M}_\odot}\right)^x. \quad \text{(A.1)}$$

Here $\left|\dot{M}_{ref}\right|$ is a reference mass loss rate and x and y are parameters that set how the mass-loss rate depends on initial and instantaneous mass, respectively (see Eq. 4 of Gieles & Gnedin 2023). These three parameters depend on $\rho_{h,0}$, relative to the tidal density, which depends on the strength of the tidal field, which is quantified by the parameter Ω_{tid}.

For a single isothermal sphere, $\Omega_{tid} = \sqrt{2}V_c/R_{eff}$, where $V_c = 220\,\mathrm{km/s}$ and $R_{eff} = R_p(1+e)$, with R_p and e the periapsis and eccentricity of the orbit of the cluster around the Galaxy, respectively. For our models, $R_p \simeq 6.5\,\mathrm{kpc}$ and $e \simeq 0.6$, so $R_{eff} = 10.5\,\mathrm{kpc}$ and $\Omega_{tid} = 0.03\,\mathrm{Myr}^{-1}$.

Gieles & Gnedin (2023) show that x, y and $\left|\dot{M}_{ref}\right|$ depend on $\rho_{h,0}$ relative to the tidal density, which can be captured by the parameter $\mathcal{R}_0 \equiv \rho_{h,0}/\rho_{h,f}$, where $\rho_{h,f} \simeq 39\Omega_{tid}^2/G \simeq 8\,M_\odot\,\mathrm{pc}^{-3}$ is the half-mass density of a tidally filling cluster on the orbit of ED-2 (see Sect. 2.1[2] in Gieles & Gnedin 2023). For $t_{dis} = 4\,\mathrm{Gyr}$ and 8 Gyr, we used at $\mathcal{R}_0 = 29$ and 95, and the corresponding values for $\left|\dot{M}_{ref}\right|$, x and y from their Table 1 to find M_0 and $\rho_{h,0}$. For $t_{dis} = 0.5\,\mathrm{Gyr}$ we used the lower $\mathcal{R}_0 = 3$, to ensure that M_0 is within the allowed range.

[2] We note that there is a typo in their expression for $\rho_{J,eff}$ on p. 5342 (left), where the 2 should be a 4.